On the front shape of an inertial granular flow down a rough incline

G. Saingier, S. Deboeuf, and P.-Y. Lagrée

Citation: Physics of Fluids **28**, 053302 (2016); doi: 10.1063/1.4948401
View online: http://dx.doi.org/10.1063/1.4948401
View Table of Contents: http://scitation.aip.org/content/aip/journal/pof2/28/5?ver=pdfcov
Published by the AIP Publishing

Articles you may be interested in

Kinetic-theory-based model of dense granular flows down inclined planes
Phys. Fluids **24**, 073303 (2012); 10.1063/1.4736738

Rapid flow of dry granular materials down inclined chutes impinging on rigid walls
Phys. Fluids **19**, 053302 (2007); 10.1063/1.2726885

Submarine granular flows down inclined planes
Phys. Fluids **17**, 103301 (2005); 10.1063/1.2069864

Granular flow down a rough inclined plane: Transition between thin and thick piles
Phys. Fluids **15**, 1 (2003); 10.1063/1.1521719

On the shape of granular fronts down rough inclined planes
Phys. Fluids **11**, 1956 (1999); 10.1063/1.870057

Reuse of AIP Publishing content is subject to the terms at: https://publishing.aip.org/authors/rights-and-permissions. Downloaded to IP: 93.28.90.210 On: Tue, 17 May 2016 06:16:51

CrossMark click for updates

PHYSICS OF FLUIDS **28**, 053302 (2016)

On the front shape of an inertial granular flow down a rough incline

G. Saingier,[1,2] S. Deboeuf,[1,a)] and P.-Y. Lagrée[1]
[1]*Sorbonne Universités, UPMC Univ Paris 06, CNRS UMR 7190, Institut Jean le Rond d'Alembert, F-75005 Paris, France*
[2]*Surface du Verre et Interfaces, UMR 125, CNRS/Saint-Gobain, 93303 Aubervilliers, France*

(Received 9 November 2015; accepted 19 April 2016; published online 6 May 2016)

Granular material flowing on complex topographies are ubiquitous in industrial and geophysical situations. In this paper, we study the small-scale experiment of a granular layer flowing on a rough incline. The shape of the granular front is solved analytically by using depth-averaged mass and momentum equations with a fractional expression for the frictional rheology $\mu(I)$, which is a generalization of Gray and Ancey ["Segregation, recirculation and deposition of coarse particles near two-dimensional avalanche fronts," J. Fluid Mech. **629**, 387 (2009)]. Unlike previous studies where a "plug flow dynamics" is assumed, a free shape factor α describing the vertical velocity profile is taken into account. The effect of inertia and shear rate on the front profile is evidenced through the introduction of the Froude number and the shape factor α. The analytical predictions are compared to experimental results published by Pouliquen ["On the shape of granular fronts down rough inclined planes," Phys. Fluids **11**, 1956 (1999)] and with our new experimental data obtained at higher Froude numbers. A good agreement between theory and experiments is found for $\alpha = 5/4$, corresponding to a Bagnold-like velocity profile. However, we observe a systematic deviation near the head of the front where the height vanishes: the theory predicts a continuous precursor layer, while a grain-free region is observed experimentally. This suggests that the vertical velocity profile is not uniform inside the front, but the shape factor α tends to 1 near the head of the front. This raises questions about the vertical velocity profile in granular flows and about the expression of the rheological function $\mu(I)$ and its calibration from experimental data. *Published by AIP Publishing.* [http://dx.doi.org/10.1063/1.4948401]

I. INTRODUCTION

The flow of granular material on inclined topographies is a fundamental situation encountered in many industrial applications (chemical or civil engineering, food-processing industry) and geophysical situations (rock avalanches, pyroclastic flows). It has motivated extensive experimental, numerical, and theoretical works based on model granular systems for several decades.[1–4] In spite of these numerous studies, no constitutive law is currently able to predict and explain all the range of behaviours exhibited by dry cohesionless granular material.[5]

The first system of closed equations for a granular flow was proposed by Savage and Hutter[6] in 1989 by depth-averaging the mass and momentum equations in 1D, and introducing a constant Coulomb basal friction law. It was then extended in 2D by Gray *et al.*[7] These theoretical models resemble the Saint-Venant shallow water equations commonly used for liquids, but with an additional source term.[8] Other derivations of these equations were performed for snow avalanches.[9,10] These approaches require some hypothesis on the shape of the normal velocity profile for the determination of the shape factor α, defined later in Eq. (5). Many authors choose to consider a "plug flow" profile (no shear), leading to a simplification of the equations. A similar problem exists for

a)Author to whom correspondence should be addressed. Electronic mail: sdeboeuf@dalembert.upmc.fr

Reuse of AIP Publishing content is subject to the terms at: https://publishing.aip.org/authors/rights-and-permissions. Downloaded to IP: 93.28.90.210 On: Tue, 17 May 2016 06:16:51

newtonian shallow water flows where the influence of the shape factor is often neglected. Nevertheless, Hogg and Pritchard[11] have shown the importance of the shape factor to correctly describe the inertial flows of viscous laminar fluids.

In 1999, Pouliquen[12] applied the same approach as Savage and Hutter[6] to explain his experimental results of granular front profiles for a steady uniform flow on an inclined plane. He used an empirical basal friction[13] instead of a constant friction. Different expressions for this friction law are now proposed in the literature.[14–18] Following these works, the local $\mu(I)$-rheology has recently emerged as an appropriate framework to describe experimental observations and discrete numerical simulations, and proved reliable when implemented in continuum numerical simulations.[1,15,19–21] In a 2D shear flow of grains of diameter d and density ρ, this formalism describes the friction coefficient μ, corresponding to the ratio of the shear stress τ and the normal stress (or pressure) P

$$\mu = \frac{\tau}{P}, \tag{1}$$

as a function of the inertia number I, depending on the pressure P and the shear rate $\dot{\gamma}$, defined as

$$I = \frac{\dot{\gamma} d}{\sqrt{P/\rho}}. \tag{2}$$

In this paper, we propose an analytical solution for the granular front of a steady uniform flow on an inclined plane, by using depth-averaged equations with the fractional $\mu(I)$-rheology as defined in Jop *et al.*[16] This is a generalization of Gray and Ancey[22] to the case $\alpha \neq 1$. By taking into account the shape of velocity profile ($\alpha \neq 1$) and the existence of shear, we will show that the front profile depends on the velocity profile and the Froude number defined in Eq. (10). This prediction is confirmed by a comparison with previous experiments from Pouliquen[12] and with our new experimental results of granular flows on a rough inclined plane at higher Froude numbers. A finer comparison of theory and experiments shows that $\alpha = 5/4$ in uniform regions but suggests that $\alpha = 1$ near the head of the front.

This paper begins in Sec. II by the introduction of the theoretical model and the determination of the analytical front profile. In Sec. III, the experimental setup, the measurement methods and the first experimental observations are presented. The comparison between experimental data and theoretical predictions is done in Sec. IV by using results from Pouliquen[12] and our new experimental results at higher Froude numbers. Finally, the results are discussed in Sec. V.

II. ANALYTICAL SOLUTION FOR THE FRONT PROFILE

We consider a thin layer, transversally uniform (or 2D), of a granular material of solid fraction ϕ composed of grains of diameter d and density ρ. We assume that the granular flow is incompressible and we will take the solid fraction equal to $\phi = 0.6$. The granular material flows over a rough inclined surface, that is assumed to impose a no-slip boundary condition at the bottom. The streamwise and vertical coordinates are denoted by x and z, and $h(x,t)$ denotes the depth of the layer. The shallowness of the granular layer allows us to use the depth-averaged equations in 1D written by Savage and Hutter,[6]

$$\frac{\partial h}{\partial t} + \frac{\partial}{\partial x}(h\bar{u}) = 0, \tag{3}$$

$$\frac{\partial}{\partial t}(h\bar{u}) + \alpha \frac{\partial}{\partial x}(h\bar{u}^2) = hg\cos\theta(\tan\theta - \mu(\bar{I}) - k\frac{\partial h}{\partial x}), \tag{4}$$

where $\bar{u}$ denotes the depth-averaged velocity. The first term of the right hand side is the gravity along the slope, the second is the basal friction, and the third is the pressure gradient. Note that here in general, we will take the earth pressure coefficient k describing the redistribution of normal stresses[7,12,23] ($\sigma_{xx} = k\sigma_{yy}$) equal to 1. However we will discuss the effect of the value of k in the discussion. We introduce the shape factor α usually defined as

Reuse of AIP Publishing content is subject to the terms at: https://publishing.aip.org/authors/rights-and-permissions. Downloaded to IP: 93.28.90.210 On: Tue, 17 May 2016 06:16:51

$$\alpha = \frac{\frac{1}{h}\int_0^h u^2(z)dz}{\left(\frac{1}{h}\int_0^h u(z)dz\right)^2}. \tag{5}$$

In many papers, the simplification $\alpha = 1$ is carried out by the authors.[6,12,24–26] This simplification implies that the material presents a uniform velocity profile in the vertical direction. The material flows like a solid without shear ("plug flow"). This assumption may be really inappropriate to describe the flow of a granular thin layer on a rough surface (with a no-slip boundary condition) regarding the Bagnold-like profile for the velocity[1] defined by

$$\frac{u(z)}{\sqrt{gd}} = \frac{2}{3}\bar{I}\sqrt{\cos\theta}\frac{(h^{3/2} - (h-z)^{3/2})}{d^{3/2}}. \tag{6}$$

For this velocity profile, the mean velocity $\bar{u} = 3u(h)/5$, where $u(h)$ is the free surface velocity and the mean inertial number $\bar{I}$ is equal to

$$\bar{I} = \frac{5}{2}\frac{\bar{u}d}{h\sqrt{\phi g h\cos\theta}}. \tag{7}$$

With this expression (6) for the velocity profile, the calculation of the shape factor leads to $\alpha = 5/4$. In this paper, we do not consider the usual simplification $\alpha = 1$ and we will discuss the effect of the value of α. The friction $\mu(I)$ is expressed here with the fractional friction law proposed by Jop *et al.*[16]

$$\mu(I) = \mu_0 + \frac{\Delta\mu}{I_0/I + 1}, \tag{8}$$

where μ_0, $\Delta\mu$, and I_0 are empirical parameters characterizing the granular setup.

With (3), (4), (8) and appropriate boundary conditions, it is possible to solve the problem for a shallow granular flow. In order to derive the analytical front profile of a steady uniform flow, we will solve this system of equations in the case of the front propagation, with the boundary condition $h = h_\infty = \text{cst}$ far upstream to the front. As observed experimentally by Pouliquen[12] (and as we will show in the next part, see Fig. 3), the front moves at a constant velocity u_0 with a steady shape, leading to a travelling wave for the front profile

$$h(x,t) = h(\xi) \text{ with } \xi = x - u_0 t. \tag{9}$$

The mass balance equation (3) becomes $d(h(\bar{u} - u_0))/d\xi = 0$, implying that $\bar{u} = u_0$ for $h \neq 0$. Far upstream to the front, the flow tends toward a steady uniform flow characterized by the thickness h_∞ and the velocity u_0. By using this change of variables ($\xi = x - u_0 t$) and by introducing the Froude number Fr[27] associated to the steady uniform flow defined as

$$Fr = \frac{u_0}{\sqrt{g h_\infty \cos\theta}}, \tag{10}$$

the depth-averaged momentum balance equation (4) can be rewritten in the moving frame as

$$\left[(\alpha - 1)Fr^2\frac{h}{h_\infty} + 1\right]\frac{dh}{d\xi} = \tan\theta - \mu(\bar{I}). \tag{11}$$

Since the depth-averaged velocity $\bar{u}$ is the same everywhere, equal to u_0, it is possible to determine it by using the Bagnold-like velocity profile Eq. (6). Here, we assume a Bagnold-like velocity profile everywhere in the granular layer. In each point of the front, the velocity u_0 is

$$u_0 = \frac{2\bar{I}_\theta}{5}\sqrt{\phi g h_\infty\cos\theta}\frac{h_\infty}{d} = \frac{2\bar{I}}{5}\sqrt{\phi g h\cos\theta}\frac{h}{d}, \tag{12}$$

where $\bar{I}$ and $\bar{I}_\theta$ are the inertia numbers associated to the flow of thickness h at the position ξ and to the steady-uniform flow of thickness h_∞ far upstream, respectively. Equation (12) leads to the relationship between $\bar{I}$ and $\bar{I}_\theta$

$$\frac{\bar{I}_\theta}{\bar{I}} = \left(\frac{h}{h_\infty}\right)^{3/2}. \tag{13}$$

Reuse of AIP Publishing content is subject to the terms at: https://publishing.aip.org/authors/rights-and-permissions. Downloaded to IP: 93.28.90.210 On: Tue, 17 May 2016 06:16:51

In the steady-uniform flow, Eq. (11) simplifies and θ can be expressed as a function of $\bar{I}_\theta$ by using the friction law

$$\tan\theta = \mu(\bar{I}_\theta) = \mu_0 + \frac{\Delta\mu}{I_0/\bar{I}_\theta + 1}. \tag{14}$$

Equations (13) and (14) allow us to replace $\bar{I}/I_0$ with a function of h/h_∞

$$\frac{\bar{I}}{I_0} = \left(\frac{h_\infty}{h}\right)^{3/2} \frac{\tan\theta - \mu_0}{\mu_0 + \Delta\mu - \tan\theta}. \tag{15}$$

By using front Eq. (11) with frictional rheology (8), by introducing relation (15) and by defining the non-dimensionalized variables

$$X = \frac{\xi(\tan\theta - \mu_0)}{h_\infty}, \quad H = \frac{h}{h_\infty}, \quad \delta = \frac{\tan\theta - \mu_0}{\Delta\mu}, \tag{16}$$

we obtain the non-dimensionalized equation for the front profile

$$\left[\frac{(\alpha-1)Fr^2}{H} + 1\right]\frac{dH}{dX} = 1 - \frac{1}{\delta + H^{3/2}(1-\delta)}. \tag{17}$$

This equation has an implicit analytical solution $X(H)$ which can be expressed as

$$X = \left[\ln\left(\frac{(1-\sqrt{H})^2}{H+\sqrt{H}+1}\right) + 2\sqrt{3}\arctan\left(\frac{2\sqrt{H}+1}{\sqrt{3}}\right) - 3(\alpha-1)Fr^2\ln\left(\frac{H^\delta}{(1-H^{3/2})^{2/3}}\right)\right] \times -\frac{1}{3(1-\delta)} - H + \zeta, \tag{18}$$

with ζ an integration constant, chosen such that the tangent to the inflexion point crosses the origin point ($X = 0$, $H = 0$). Other choices are possible that will only translate the front profile along x without changing its shape. So that $h/h_\infty = X^{-1}[x(\tan\theta - \mu_0)/h_\infty]$. This solution (18) is a generalization to the case $\alpha \neq 1$ of the one proposed by Gray and Ancey[22] (Eq. (2.20)), different from the one proposed by Pudasaini[28] determined with the Bagnold's inertial stress.[29] Our non-dimensionalized solution only depends on three parameters: δ accounting for the slope angle and the rheology, Fr for the inertia, and α for the shape of the velocity profile and the existence of shear.

This solution (18) presents an asymptotic exponential behaviour when H tends to zero, for all values of α except for $\alpha = 1$.[30] Consequently, the analytical granular front for $\alpha \neq 1$ is preceded by a continuous precursor layer having to exist over the whole domain, which is not observed in experiments. This suggests that α may tend to 1 at the flow front to have grain-free regions as observed experimentally.

Recently, the depth-averaged equations have been revisited by Gray and Edwards[26] as an alternative of the equations of Forterre.[31] They obtained an extra longitudinal viscous term in Eq. (4): $\partial_x(\nu_F h^{3/2}\partial_x\bar{u})$, with $\partial_x f \equiv \partial f/\partial x$, consistent with Forterre's stability analysis.[31] Gray and Edwards[26] demonstrated that their term does not change anything in the case of the front (even in our model with $\alpha \neq 1$) because $\bar{u}$ is constant, whereas Forterre's term predicts a continuous precursor layer exponentially decreasing. They proposed that this unphysical behavior advocates for their viscous term. In our case, we have an exponential decay as well with $\alpha \neq 1$, which suggests that α may tend to 1 at the flow front.

The effect of different parameters on the front profile is discussed in Fig. 1. Fig. 1(a) shows several fronts for Froude numbers Fr increasing from 0 to 3.2 for a slope angle $\theta = 27°$ and $\alpha = 5/4 = 1.25$ (Bagnold-like velocity profile). The non-dimensionalized front shape is flattened down by the inertial term and the size of the precursor layer increases when the Froude number Fr increases. In Fig. 1(b), front profiles are plotted at a constant $Fr = 2.0$ for different values of α between 1 and $4/3 = 1.33$ for a slope angle $\theta = 27°$. An increase of α also implies the flattening of the front. The "plug flow" profile corresponds to $\alpha = 1$. The case $\alpha = 5/4 = 1.25$ represents a Bagnold-like velocity profile whereas for $\alpha = 4/3 = 1.33$, the velocity profile is linear and for

Reuse of AIP Publishing content is subject to the terms at: https://publishing.aip.org/authors/rights-and-permissions. Downloaded to IP: 93.28.90.210 On: Tue, 17 May 2016 06:16:51

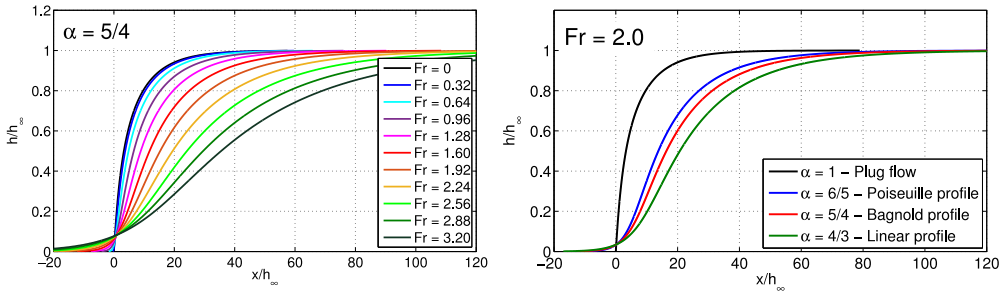

FIG. 1. Analytical solution for the front profile plotted for several sets of parameters at the slope angle $\theta = 27°$: (left) effect of the Froude number Fr for $\alpha = 5/4$; (right) effect of the shape factor α for $Fr = 2.0$: $\alpha = 1,\ 6/5 = 1.20,\ 5/4 = 1.25$ and $4/3 = 1.33$.

$\alpha = 6/5 = 1.20$, the profile corresponds to a Poiseuille flow. The continuous precursor layer exists for all values of $\alpha \neq 1$ (and $Fr \neq 0$) and the only case for having a grain-free region is for $\alpha = 1$ (or $Fr = 0$).

Finally, considering the simplification $\alpha = 1$ implies to vanish all the terms which contain Fr. The analytical solution (18) can be reduced by choosing $\alpha = 1$ or $Fr = 0$, to the solution

$$X = \left[\ln\left(\frac{(1-\sqrt{H})^2}{H+\sqrt{H}+1}\right) + 2\sqrt{3}\arctan\left(\frac{2\sqrt{H}+1}{\sqrt{3}}\right)\right] \times -\frac{1}{3(1-\delta)} - H + \zeta, \tag{19}$$

with ζ an integration constant chosen such that $X = 0$ for $H = 0:\ \zeta = \pi/3\sqrt{3}(\delta - 1)$. This result was published before by Gray and Ancey[22] (Eq. (2.20)). Consequently, the analytical solution for $\alpha = 1$ only depends on the slope angle and the choice of rheology parameters, through the parameter δ. The precursor layer disappears and it is possible to measure a contact angle θ_c of the profile between the granular fluid and the plane, which depends on the slope angle and the rheology parameters: $\theta_c = \arctan((\mu_0 + \Delta\mu) - \tan\theta)$.

III. EXPERIMENTAL SETUP

In order to check our theoretical predictions, we have revisited the experiments proposed by Pouliquen.[12] The propagation of the front of a dry granular material has been investigated experimentally thanks to classical experiments of inclined planes.[12,13] The setup, shown on Fig. 2, is a 2-m-long and 40-cm-wide rough plane (from Norcan) which can be inclined at the desired slope angle. The granular material is stored in a reservoir at the top of the plane and is released through a gate which can be opened quickly and precisely. A second gate allows to adjust the aperture thickness in order to control the mass flow rate. The rough surface is obtained by gluing the same flowing particles on the plane (to ensure a no-slip boundary condition at the bottom).

The granular material and the glued layer are composed of quasi monodispersed spherical glass beads of diameters $d = 200 \pm 50\ \mu$m (from Marteau & Lemarié) and the solid fraction is taken equal to $\phi \approx 0.60$. The size of particles is small enough in comparison with the size of the granular layer ($\approx$1 cm) to justify the hydrodynamical continuous model used previously in Section II.[1] Side walls are polyethylene plates to guarantee that the lateral conditions are not very rough. In our experiments, only the centerline of the granular flow is studied to be assimilated to a 2D flow.

For the range of slope angles (25°–30°) and aperture thicknesses (5 mm–30 mm) that we have studied, a granular front hurtles down the slope at constant velocity with a steady shape, as shown in Fig. 3. The front velocity u_0 is measured by tracking the front propagating down the inclined plane with a home-made program based on thresholding in Matlab or with time-space graphs in ImageJ using the reslice command. We observe that u_0 is constant during the propagation of the front. The thickness of the steady-uniform flow and the shape of the front are measured in a region of size $\approx$60 cm at a distance of 1 m from the aperture in order to be unaffected by the transient region near the gate. The method of measurement consists to illuminate longitudinally the flow surface

Reuse of AIP Publishing content is subject to the terms at: https://publishing.aip.org/authors/rights-and-permissions. Downloaded to IP: 93.28.90.210 On: Tue, 17 May 2016 06:16:51

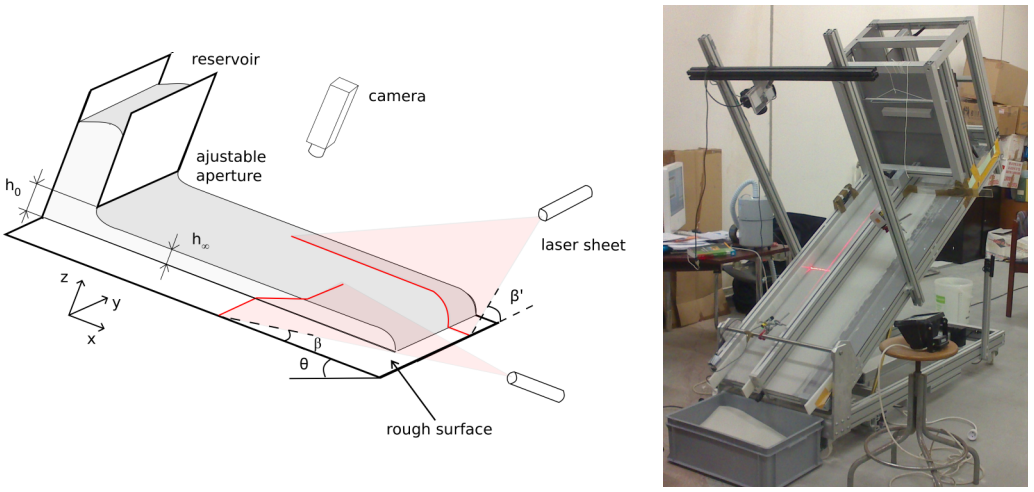

FIG. 2. Experimental setup: (left) Schematic representation of the setup; (right) Photograph of the setup.

with a laser light sheet at a low incident angle (see Pouliquen[13]). Where the granular flow crosses the projection of the laser sheet, it is shifted laterally from the initial position. The lateral shift is proportional to the thickness $h_t(x)$ and can be determined precisely after calibration. The spatial front profile at different times is plotted in Fig. 3(a). The superposition of front profiles separated by times Δt when translated by distances $\Delta x = u_0 \Delta t$ shows experimentally that the velocity of the front is constant during the propagation and the front propagates with a steady shape, as a progressive wave (see Fig. 3(b)). This is in accordance with what was theoretically assumed before in Section II. A second laser sheet illuminates the surface transversally with a smaller incident angle (see Deboeuf *et al.*[32]). Thus we obtain the transversal thickness at a position $x(t)$. By doing this measurement at several times, it is possible to determine a temporal evolution of the thickness $h_x(t)$. A comparison of both profiles ($h_t(x)$ and $h_x(t)$) is possible, thanks to the change of variables $t \rightarrow x = u_0 t$ or $x \rightarrow t = x/u_0$. As shown by the superposition of the spatial and temporal profiles on Fig. 3(b), this method of transversal profilometry leads to the same profile that the longitudinal profilometry, allowing for a higher resolution on a longer region of observation. It also proves that $\overline{u} = u_0$ in each position x of the flow, showing that everything is actually constant in the moving frame. Lastly, we systematically check the superposition of spatial and temporal fronts for our different control parameters.

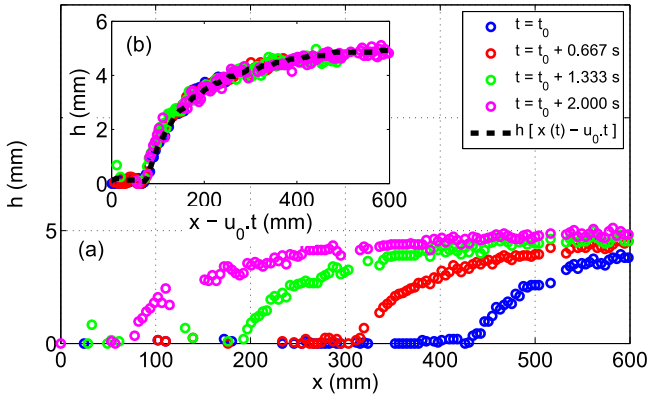

FIG. 3. (a) Granular front propagating at several times. (b) Superposition of the front profiles at different times by the change of variable $\xi = x - u_0 t$. The profiles obtained with spatial data are presented in filled circles, whereas the temporal front is shown with the dashed line after the variable change $t \rightarrow x = u_0 t$. $\theta = 25.2°$, $h_\infty = 4.9$ mm and $u_0 = 18$ cm/s.

Reuse of AIP Publishing content is subject to the terms at: https://publishing.aip.org/authors/rights-and-permissions. Downloaded to IP: 93.28.90.210 On: Tue, 17 May 2016 06:16:51

Let us now compare experimental results with the theoretical ones by using previous experimental results from Pouliquen[12] and our new experimental data at higher Froude numbers.

IV. RESULTS

A. First case: Small Froude numbers or no shear hypothesis ($\alpha = 1$)

First, we consider the case of slow granular flows ($Fr \simeq 0$). In this case, the inertial term can be neglected and the front equation (11) simplifies to give the equation[7,12]

$$\frac{dh}{d\xi} = \tan\theta - \mu(\bar{I}). \tag{20}$$

The same equation is deduced if we consider $\alpha = 1$ as assumed in many papers,[6,12,22,26,33] or more generally if $(\alpha - 1)Fr^2 h/h_\infty \ll 1$. Consequently, even if this simplification ($\alpha = 1$) is not physically justified for granular Bagnold-like flows, it leads surprisingly and fortuitously to a coherent equation for slow granular flows on rough inclines.

Pouliquen[12] presented experimental results of granular material flowing on a rough inclined plane. He observed a good collapse of experimental data of front profiles $h(x)$ when rescaling h and x by the steady-uniform thickness h_∞. The equation (20) has been solved numerically by Pouliquen[12] with an exponential frictional rheology:[13] $\mu(I) = \mu_0 + \Delta\mu \exp(-I_0/I)$. More recently, Gray and Ancey[22] solved it analytically with fractional rheology (8) and obtained expression (19). Note that the extended formulation of depth-averaged equations with viscous terms[26] made no difference to the front shape, whereas other formulations[31] lead to similar problems of a precursor layer, this time due to the form of the depth-averaged viscous terms.

In this analytical expression (19), the profile only depends on the parameter δ which depends on the slope angle θ and the rheology parameters μ_0 and $\Delta\mu$ (and not I_0). Consequently, for an imposed slope angle θ, the profiles are the same after dividing h and x by h_∞, as observed for the experimental data of Pouliquen.[12]

Fig. 4 is extracted from Pouliquen[12] and presents some experimental data obtained for one size of beads ($d = 500$ μm, system 4[13]). The solution calculated for $\alpha = 1$ with the fractional form of the $\mu(I)$ rheology (Eq. (19)) is superimposed (in black line) on the numerical solution proposed by Pouliquen with the exponential form. Our analytical solutions calculated for $\alpha = 5/4$ (Eq. (18)) have been computed and also superimposed (in color lines) to experimental data. To compute them, we needed the rheological parameters that we characterized by fitting $h_{stop}(\theta)$ data[13] and fitting the flow rule $u/\sqrt{gh}(h/h_{stop})$.[12] We observe that the profiles are only slightly flattened but stay in the error bars of the experimental data. Both of the predictions ($\alpha = 1$ and $\alpha = 5/4$) well describe his experimental data. Indeed the range of velocity of these granular flows (from 2 to 20 cm/s)

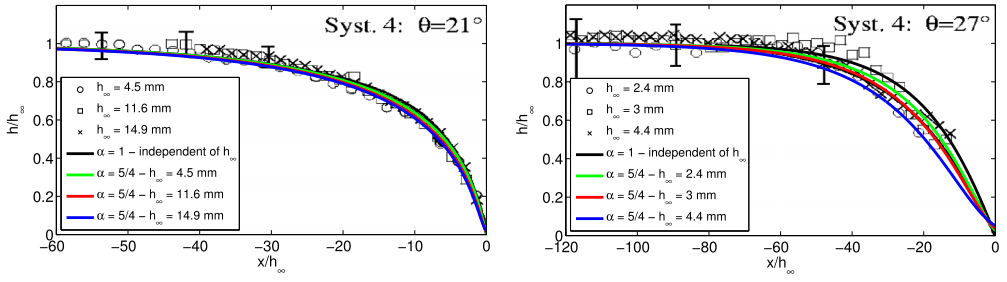

FIG. 4. Front profiles from Pouliquen:[12] comparison between experiments for different h_∞ (symbols) and theory obtained with the fractional rheology (solid lines). Colored and dark lines correspond to the calculations with $\alpha = 5/4$ and $\alpha = 1$, respectively. The curves for $\alpha = 1$ with a fractional expression for the rheology are superimposed on the numerical fronts obtained by Pouliquen with an exponential expression. Rheology parameters are determined by fitting $h_{stop}(\theta)$ data from Pouliquen:[13] $\mu_0 = 0.35$ and $\Delta\mu = 0.21$. Froude numbers were determined by fitting the flow rule $u/\sqrt{gh}(h/h_{stop})$ data from Ref. 12.

Reuse of AIP Publishing content is subject to the terms at: https://publishing.aip.org/authors/rights-and-permissions. Downloaded to IP: 93.28.90.210 On: Tue, 17 May 2016 06:16:51

corresponds to small Froude numbers since the typical thickness of the flow is 1 cm (from $Fr = 0.1$ to $Fr = 1$). Consequently, the simplification leading to Eq. (20) is relevant.

B. Second case: Inertial effect at higher Froude numbers ($\alpha \neq 1$)

Now we consider the case of granular flows at larger Froude numbers, or more generally when $(\alpha - 1)Fr^2 h/h_\infty \sim 1$. The inertial term cannot be neglected anymore in Eqs. (4) and (11). This term adds a dependence of the front profile on the Froude number Fr and the velocity profile through the value of α.

We have realized new experiments with the setup described in Sec. III, allowing us to explore a wider range of velocities, from 10 to 80 cm/s (from $Fr = 0.5$ to $Fr = 3$) and to study the effect of inertia. Some raw data of front profiles are presented in Fig. 5 for slope angles $\theta = 26.2°$, $27.2°$, $28.2°$, and $29.2°$ and for steady heights 4.4 mm $< h_\infty <$ 11 mm. The thickness h_∞ is measured with a precision of ±0.5 mm. When rescaling h and x by h_∞ at a given slope, the data of front profiles do not collapse on a single curve, as expected for non-inertial flows (or for $\alpha = 1$), but sort according to the front velocity, as shown in Fig. 6. The flattening of the front for increasing Froude numbers can be observed, as theoretically expected for $\alpha \neq 1$. By plotting the analytical solutions computed for $\alpha = 5/4 = 1.25$ (Bagnold-like profile), we have observed a good agreement between our experimental data and our theoretical predictions. Moreover, the profile computed with $\alpha = 1$ is systematically above the other curves (see Fig. 6), which proves that the hypothesis of a "plug flow" profile everywhere in the layer is not adapted to describe the front of a granular flow on inclines at moderate or large Froude numbers.

However, we observe systematically an obvious discrepancy between analytical and experimental fronts in the vicinity of $h \simeq 0$: the theory predicts a continuous and infinite precursor layer whereas experiments show a grain-free region. The only way to have a grain-free region near the head of the front is to have here $\alpha = 1$, suggesting here a "plug flow." As a conclusion, the velocity profile does change inside the layer, starting from a Bagnold-like profile in uniform regions where $h = h_\infty$ to a constant profile near the head of the front where $h \simeq 0$.

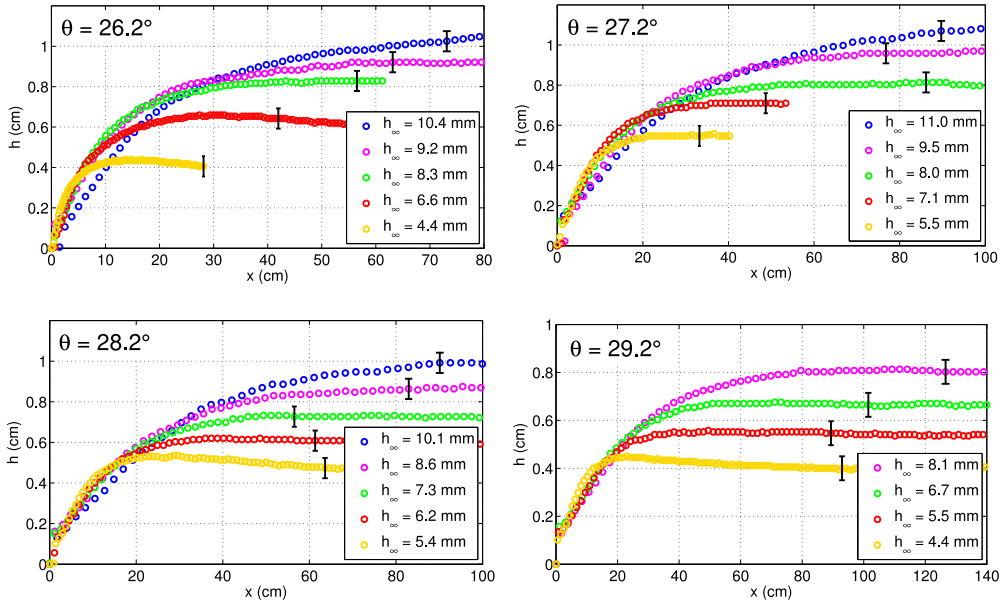

FIG. 5. Granular front profiles measured experimentally by transversal laser profilometry for different slope angles $\theta = 26.2°$, $27.2°$, $28.2°$, and $29.2°$ and different thicknesses h_∞ from 4.4 mm to 11.0 mm, controlled by the aperture of the gate.

Reuse of AIP Publishing content is subject to the terms at: https://publishing.aip.org/authors/rights-and-permissions. Downloaded to IP: 93.28.90.210 On: Tue, 17 May 2016 06:16:51

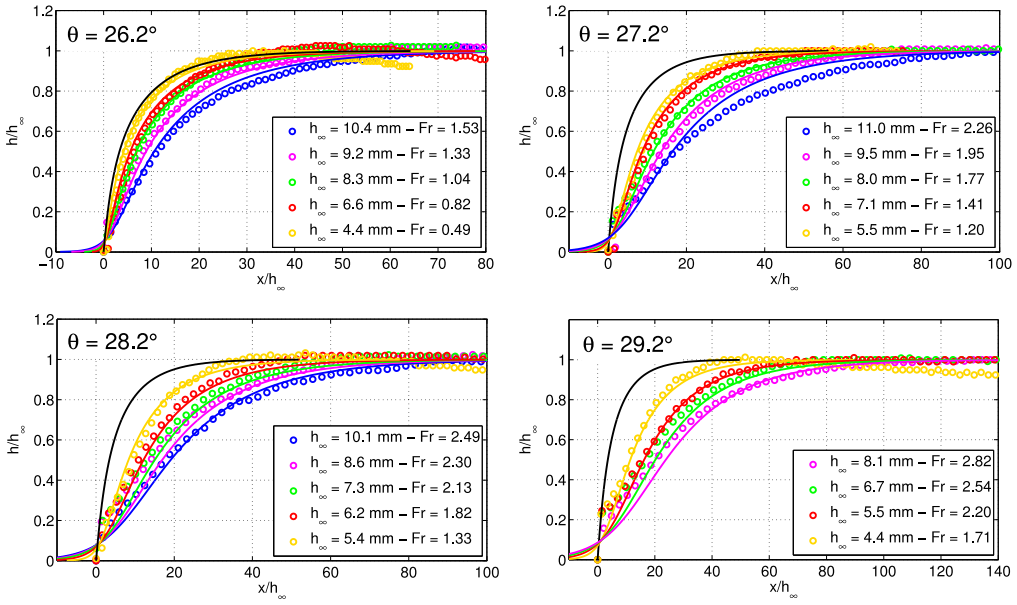

FIG. 6. Rescaled granular profiles: comparison between experiments and analytical predictions for different slopes and thicknesses h_∞. Analytical solutions (colored lines) are calculated by using the thickness h_∞ and the front velocity u_0 measured for each experimental front (colored circles) with a shape factor $\alpha = 5/4$. The analytical solution evaluated for $\alpha = 1$ is plotted in black line. Theoretical solutions are computed with rheology parameters $\mu_0 = 0.41$ and $\Delta\mu = 0.35$, determined by fitting our h_{stop} data.

V. DISCUSSION

In this paper, we have generalized the analytical solution[7] for the front profile of a steady uniform flow on an incline[22] obtained from depth-averaged equations with the fractional frictional rheology $\mu(I)$ to the case of a shape factor $\alpha \neq 1$ accounting for a non-constant vertical velocity profile (different from a "plug flow"). This model has been compared with experimental data, demonstrating the role of inertia and the influence of the free shape factor α on the front profile. In this section, we will discuss the influence of different parameters on the front profile. In a first part, we will study the influence of non-isotropic normal stresses in the granular material ($k \neq 1$); in a second part, we will focus on the choice of the velocity profile used to compute the analytical solutions; and in a third part, we will analyze the effect of the rheology on our model.

A. Influence of the earth pressure coefficient

If assuming non-isotropic normal stresses in the granular material, that is $k \neq 1$, where k is the earth pressure coefficient such that $\sigma_{xx} = k\sigma_{yy}$, the main equation for front Eq. (11) becomes

$$\left[(\alpha - 1)Fr^2\frac{h}{h_\infty} + k\right]\frac{dh}{d\xi} = \tan\theta - \mu(\bar{I}), \tag{21}$$

leading to the analytical solution for the non-dimensionalized front profile

$$X = \left[k\ln\left(\frac{(1-\sqrt{H})^2}{H+\sqrt{H}+1}\right) + 2k\sqrt{3}\arctan\left(\frac{2\sqrt{H}+1}{\sqrt{3}}\right) - 3(\alpha-1)Fr^2\ln\left(\frac{H^\delta}{(1-H^{3/2})^{2/3}}\right)\right] \times -\frac{1}{3(1-\delta)} - kH + \zeta, \tag{22}$$

with ζ an integration constant chosen such that the tangent to the inflexion point crosses the origin point ($X = 0$, $H = 0$). The Mohr-Coulomb theory predicts for the value of the earth pressure coefficient $k = (1 + \sin^2\theta_c)/(1 - \sin^2\theta_c) \geq 1$, with θ_c, an internal friction angle, equal here to $k = 1.3$

Reuse of AIP Publishing content is subject to the terms at: https://publishing.aip.org/authors/rights-and-permissions. Downloaded to IP: 93.28.90.210 On: Tue, 17 May 2016 06:16:51

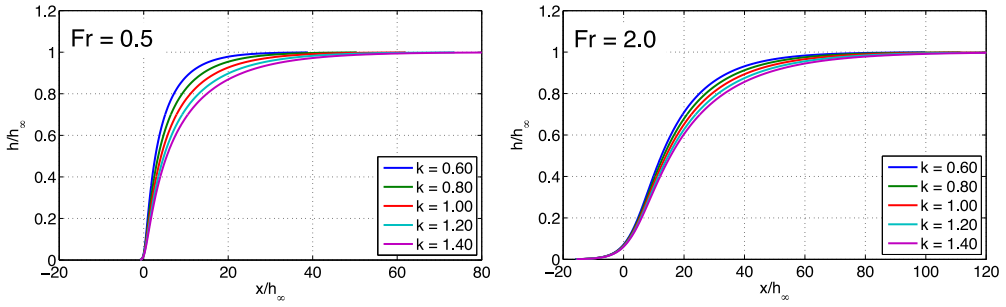

FIG. 7. Influence of the value of the earth pressure coefficient k on the front profile for a slope angle $\theta = 27°$ for two Froude numbers ($Fr = 0.5$ on the left and $Fr = 2.0$ on the right): k changes between 0.60 and 1.40.

if assuming it equal to the static basal friction, i.e., $\tan\theta_c = \mu_0$, as done in Ref. 13. Figure 7 show different front profiles for k varying from 0.60 to 1.40 for two different Froude numbers (0.5 and 2). Increasing the value of k tends to flatten the front profiles. However this effect is less and less visible for increasing Froude numbers. The experiments and the theoretical predictions of Pouliquen[12] show that $k = 1$ (solid line of Fig. 3 in Ref. 12) describes well the experimental data, while a constant k from the Mohr-Coulomb theory (dashed line of Fig. 3 in Ref. 12) still stays within the error bars. Moreover, numerous works on flows past obstacles[34,35] tends to confirm that $k = 1$ and invalidate that k switches from active to passive earth pressure coefficients. Lastly, the isotropy of normal stresses (and the relevance of a pressure) or the existence of a shift of normal stresses, possibly dependent on the shear rate as in dense suspensions,[36–38] is still a matter of debate.[39,40]

B. Influence of the velocity profile

In this work, we have shown the importance of the vertical velocity profile in order to describe finely the shape of the front of a flowing granular layer. Contrary to many papers in the literature,[6,12,22,24–26,33] we have chosen a shape factor non-equal to 1 ($\alpha \neq 1$), describing shear in the granular layer. Indeed, in the case of a steady uniform granular flow on an inclined plane with a no-slip boundary condition at the bottom, we can demonstrate that the velocity profile should follow the Bagnold-like profile in uniform regions.[1] Consequently, for a comparison of our experimental results and our theoretical computations, we have supposed that this velocity profile was established in each point of the layer. This hypothesis may be not satisfactory everywhere, in particular in the head of the front, which is greatly non-uniform and out of the theoretical Bagnold's limits. Note that experimental and numerical data report some deviations from the Bagnold-like profile even in the steady-uniform flow. In particular, results from Deboeuf *et al.*[32] show that the ratio between the mean velocity and the surface velocity for steady-uniform granular flows can change in function of the thickness. This ratio increases from 1/2 for thicknesses close to h_{stop} to 3/5 for thicker flows, which would correspond to linear and Bagnold-like profiles, respectively (shape factors α equal to 4/3 and 5/4, respectively). This tendency is confirmed by discrete numerical simulations,[1,39,41,42] which show that the vertical velocity profile is a Bagnold-like profile in thick flows, whereas it is linear in thin flows. This raises the question of the non-universality of a Bagnold-like profile for a steady and uniform flow on an incline. One possible reason would be the non-generality of the no-slip boundary condition at the base. The role of the base roughness on the dynamics and on the boundary condition of the flow is not so clear as well. However, in the range of thicknesses experimentally explored in this work, the hypothesis of a Bagnold-like profile seems acceptable.

Nevertheless, by choosing a value for α different than 1, we have observed that the analytical solution presents an inflexion point near the head of the front, which leads to a continuous precursor layer. Experimental observations seem to invalidate this precursor layer. For small Froude numbers, the front surface is well defined and does make a finite contact angle with the plane (see Fig. 5 for $\theta = 26.2°$). For higher Froude numbers, the precision of measurements for $h \simeq 0$ is reduced due to splashes of grains downstream of the front (see Fig. 5 for $\theta = 27.2°$, $28.2°$, and $29.2°$). These

Reuse of AIP Publishing content is subject to the terms at: https://publishing.aip.org/authors/rights-and-permissions. Downloaded to IP: 93.28.90.210 On: Tue, 17 May 2016 06:16:51

splashes prevent a precise measurement of a contact angle but cannot be assimilated to a precursor layer. All these results may indicate that the velocity profile is different in the head of the front from a Bagnold-like profile and should be close to a plug flow to avoid a continuous precursor layer and allow a grain-free region. As mentioned by Hogg and Pritchard[11] for liquids, the introduction of a non-constant shape factor α may solve this issue and lead to a best agreement between analytical solutions and experimental measurements near the head of the front. This method is commonly used in fluid mechanics where equations can admit a family of solutions for a family of velocity profiles.[43] Alternatively, to regularize this asymptotic behaviour, we could introduce a cut-off length that would correspond to the size of a few grains, for instance, as it is done in fluid mechanics.[44]

To finish, we have highlighted the inconsistency of assuming $\alpha = 1$ in depth-averaged equations to describe granular flows on inclines with a no-slip boundary condition. However, after writing here the equations for $\alpha \neq 1$ in the case of the steady propagation with a steady shape of the granular front, it appears that this computation ($\alpha = 1$) is equivalent to neglect inertia ($Fr \simeq 0$). Thus this work gives a justification to this crude approximation ($\alpha = 1$). We may wonder to which extent this approximation can provide good results in other cases. On one side, the description of slow gravitational flows does not need to take into account the value of α since the dynamics is controlled by gravity and friction. On the other side, the high speed avalanche flow is a situation where inertia is important but with a significant slip at the base. In this case, the choice of a "plug flow" for the velocity profile seems appropriate and gives good results with $\alpha = 1$.[34]

C. Influence of the rheology parameters

Our analytical solution for the front profile when $\alpha \neq 1$ (Eq. (18)) is written for the friction law $\mu(I)$ expressed with the fractional expression (8), characterized by three parameters μ_0, $\Delta\mu$, and I_0. However, the rescaled profiles h/h_∞ versus x/h_∞ (Eq. (18)) do not depend on I_0: only two parameters—μ_0 and $\Delta\mu$—control the non-dimensionalized front shape. The sensibility on each parameter is evaluated by plotting front profiles for several values of μ_0 and $\Delta\mu$ in Fig. 8 for $\theta = 29°$. On this figure we put large variations (± 0.1) of μ_0 and $\Delta\mu$ for sake of illustration of their effect. Finally the value of I_0 only selects the steady thickness of the flow h_∞.

For historical reasons (see below), the friction law for a given granular system is usually deduced from fitting $h_{stop}(\theta)$ and $Fr(h/h_{stop})$ experimental data. The range of measured h_{stop} data is generally restricted (between 1 and 10 grain diameters, see Fig. 9, left) and fits usually used (fractional or exponential) are very sensitive to small values of h_{stop}. Consequently, the calibration of the rheology is sensitive to the precision and the error bar of data. In particular, an error corresponding to one size of grain can cause significant variations on the rheological parameters and modify the front morphology (see Fig. 8). This sensitivity could be overtaken if the rheological

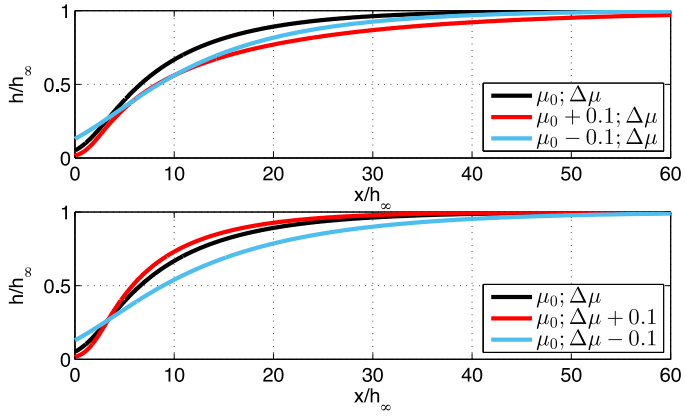

FIG. 8. Sensibility of the front profile (for $\alpha = 5/4$) to variations of the rheological parameters μ_0 and $\Delta\mu$. Black curves are plotted for the slope angle $\theta = 29°$ with $\mu_0 = 0.41$ and $\Delta\mu = 0.35$, while other colored curves are for $\mu_0 \pm 0.1$ and $\Delta\mu \pm 0.1$ at constant $\Delta\mu$ and μ_0, respectively.

Reuse of AIP Publishing content is subject to the terms at: https://publishing.aip.org/authors/rights-and-permissions. Downloaded to IP: 93.28.90.210 On: Tue, 17 May 2016 06:16:51

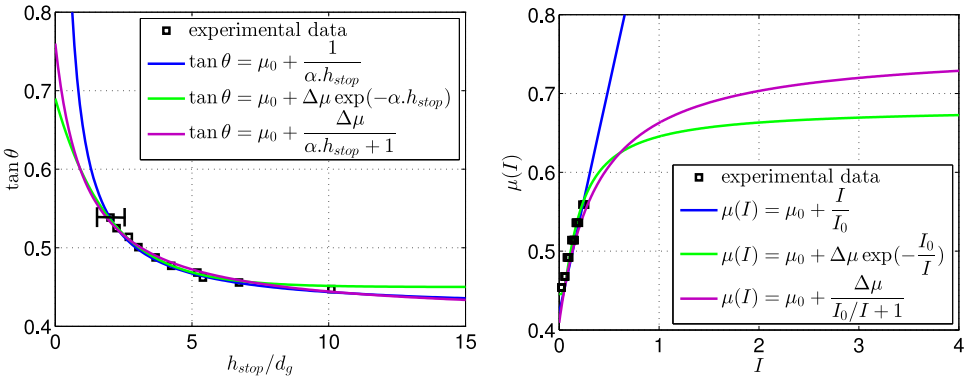

FIG. 9. Empirical determination of the rheological parameters: (left) Experimental data (square symbols) of thickness h_{stop} (plotted in x) versus θ (plotted in y) fitted by different expressions (solid lines). (right) Frictional rheology $\mu(I)$ deduced from $h_{stop}(\theta)$ fits with different expressions (solid lines) and experimental data from our steady uniform flows (square symbols). Linear: $\mu(I) = \mu_0 + I/I_0$ with $\mu_0 = 0.42$ and $I_0 = 1.73$. Exponential: $\mu(I) = \mu_0 + \Delta\mu\exp(-I_0/I)$ with $\mu_0 = 0.45$, $\Delta\mu = 0.24$ and $I_0 = 0.17$. Fractional: $\mu(I) = \mu_0 + \Delta\mu/(1 + I_0/I)$ with $\mu_0 = 0.41$, $\Delta\mu = 0.35$ and $I_0 = 0.38$.

parameters have physical interpretations (e.g., static and dynamic friction coefficients for μ_0 and $\mu_0 + \Delta\mu$). However, when experimental data of $h_{stop}(\theta)$ are fitted either by the fractional expression $\mu_0 + \Delta\mu/(1 + I_0/I)$ (Eq. (8)) or by the exponential expression $\mu_0 + \Delta\mu\exp(-I_0/I)$ as 2 examples, the values of friction parameters μ_0 and $\mu_0 + \Delta\mu$ are not the same, preventing to generalize any definition of these fit-dependent parameters (see Fig. 9, left). This raises the open question of a fine calibration of the frictional rheology from experimental data and of the theoretical framework for the expression of the function $\mu(I)$.

Let us come back to the calibration of the friction law for a granular setup. A major work, precursor of the friction law, was published by Pouliquen[13] reporting one relation between h_{stop} and θ and another relation between Fr and h/h_{stop}, allowing him to write the basal friction coefficient $\mu(I)$ from the parameters of these two relations. This indirect method is usually used to determine the relation $\mu(I)$, especially for grains flowing on an incline. One paradox of this method is the use of $h_{stop}(\theta)$ data, whereas the rheology $\mu(I)$ does not predict the existence of a deposit or a threshold thickness depending on the slope, but instead predicts the existence of one slope threshold to have a granular flow. Another way of determining the expression of $\mu(I)$ would be to fit data of μ and I without using the two previous relations, which would be a direct measurement of $\mu(I)$.

To date there is nor consensus neither theoretical arguments leading to one unique expression for the friction law (note that a theoretical background is proposed for the non-linear viscous rheology of a dense flow of frictionless spheres in a fluid[45]). Instead, we find mainly in the literature 3 different functions,

$$\mu_0 + \frac{\Delta\mu}{I_0/I + 1},\ \mu_0 + \Delta\mu\exp(-I_0/I),\ \mu_0 + I/I_0. \tag{23}$$

In Fig. 9 we show fits of $h_{stop}(\theta)$ data with these different expressions and the deduced relations for $\mu(I)$ compared to the experimental data of $\mu(I)$ coming from steady uniform flows. By doing this, we can note, in Fig. 9, right, that the range of I-values experimentally explored is not wide ($0.1 < I < 0.5$). We understand better that extending the rheology $\mu(I)$ measured from steady uniform flows to unsteady non-uniform flows was challenging for at least two reasons: because of the introduction of unsteady and non-uniform terms in mass and momentum equations and because the values of inertia numbers may be outside the range of measurements of I used for the calibration. An alternative would be to use experimental measurements of $\mu(I)$ on a wider range of I, from unsteady and/or non-uniform configurations (such as granular collapses, as studied by Lajeunesse *et al.*[46]). It should be possible from data of front profiles too by using Eq. (11): $\mu(I) = \tan\theta - \left[(\alpha - 1)Fr^2 h_\infty/h + 1\right] dh/d\xi$, which can be written for small Froude numbers (or for $\alpha = 1$) as $\mu(I) \approx \tan\theta - dh/d\xi$ (Eq. (20)). To this aim, we see that it is crucial to know α everywhere in the front. Fig. 10 shows data points from a set of experiments realized at the same slope

Reuse of AIP Publishing content is subject to the terms at: https://publishing.aip.org/authors/rights-and-permissions. Downloaded to IP: 93.28.90.210 On: Tue, 17 May 2016 06:16:51

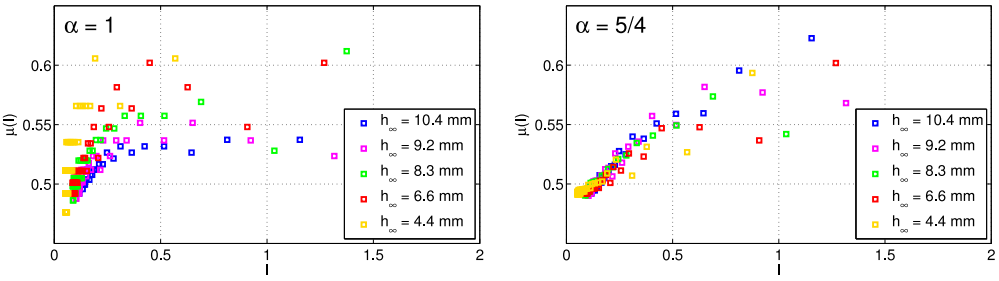

FIG. 10. Measurements of $\mu(I)$ from experimental front profiles at $\theta = 26.2°$ using Eqs. (20) and (11) for $\alpha = 1$ and $\alpha = 5/4$, respectively. For $\alpha = 5/4$, the inertia number I is computed from Eq. (7); for $\alpha = 1$, then $I = (\overline{u}d)/(h\sqrt{\phi g h \cos\theta})$, with $\phi = 0.6$ for the solid fraction.

($\theta = 26.2°$) assuming $\alpha = 1$ (left) and $\alpha = 5/4$ (right). For $\alpha = 5/4$, data better collapse for several thicknesses whereas they do not for $\alpha = 1$, especially for small I and μ, corresponding to uniform regions of h, where a Bagnold-like profile is expected. However, for larger I and μ, where h is non-uniform, the data still do not collapse with $\alpha = 5/4$. Again, this suggests that α is not constant everywhere in the flowing layer and this raises the need to measure α.

VI. CONCLUSION

We propose a theoretical model to describe the shape of a granular front of a steady uniform flow on an incline with a no-slip boundary condition. This model consists of the depth-averaged equations in 1D by considering a general velocity profile instead of a "plug flow" in the granular layer. By using a Bagnold-like velocity profile or more generally $\alpha \neq 1$, we demonstrate that inertial terms generate a front flattening at large Froude numbers. However, we also predict a continuous precursor layer which is not observed in the experiments. This suggests that $\alpha \simeq 1$ close to the head of the front where $h \simeq 0$.

Our model was first compared to experimental data coming from Pouliquen.[12] This case corresponds to small Froude numbers hence inertial effects are negligible. By rescaling experimental fronts for a given slope, data collapse onto one single curve. Taking into account the inertial corrections does not affect the front profiles significantly. We provide new experimental results at higher Froude numbers which highlight the effect of inertia, which was neglected in previous models.[6,12] A good agreement is found when comparing experimental data and theoretical predictions by assuming a Bagnold-like velocity profile established everywhere in the layer, except for $h \simeq 0$ where the theory predicts a continuous precursor layer in contradiction with experiments showing a grain-free region.

This work may be useful in the geophysical context where depth-averaged models are used to compare numerical and natural scale front deposits.[25,47]

These conclusions motivate further experimental investigations in order to determine the velocity field inside a granular front. Other approaches would consist to investigate granular fronts with discrete numerical simulations[48] or continuous numerical simulations.[20,21,49]

ACKNOWLEDGMENTS

The authors would like to thank O. Pouliquen for sharing his experimental data and for stimulating discussions, O. Dauchot, S. Popinet, and C. Josserand for stimulating discussions, and A. Lucquiaud for his preliminary work on the subject. Finally, we thank the two anonymous referees for helping us to improve our manuscript and L. Staron for her suggestions on the manuscript.

[1] G. MiDi, "On dense granular flows," Eur. Phys. J. E **14**, 341–365 (2004).
[2] J. Duran, *Sands, Powders, and Grains: An Introduction to the Physics of Granular Materials* (Springer Science & Business Media, 2012).
[3] B. Andreotti, Y. Forterre, and O. Pouliquen, *Granular Media: Between Fluid and Solid* (Cambridge University Press, 2013).
[4] R. Delannay, A. Valance, A. Mangeney, O. Roche, and P. Richard, "Granular and particle-laden flows: From laboratory experiments to field observations," J. Phys. D: Appl. Phys. (submitted).

Reuse of AIP Publishing content is subject to the terms at: https://publishing.aip.org/authors/rights-and-permissions. Downloaded to IP: 93.28.90.210 On: Tue, 17 May 2016 06:16:51

[5] Y. Forterre and O. Pouliquen, "Flows of dense granular media," Annu. Rev. Fluid Mech. **40**, 1–24 (2008).
[6] S. B. Savage and K. Hutter, "The motion of a finite mass of granulat material down a rough incline," J. Fluid Mech. **199**, 177–215 (1989).
[7] J. Gray, M. Wieland, and K. Hutter, "Gravity-driven free surface flow of granular avalanches over complex basal topography," Proc. R. Soc. A **455**, 1841–1874 (1999).
[8] A. B. de Saint-Venant, "Théorie du mouvement non permanent des eaux, avec application aux crues des rivières et à l'introduction des marées dans leurs lits," C. R. Acad. Sci. Paris **73**, 237–240 (1871).
[9] A. Kulikovskii and M. Eglit, "Two-dimensional problem of the motion of a snow avalanche along a slope with smoothly changing properties," J. Appl. Math. Mech. **37**(5), 792–803 (1973).
[10] B. Salm, "A short and personal history of snow avalanche dynamics," Cold Reg. Sci. Technol. **39**, 83–92 (2004).
[11] A. J. Hogg and D. Pritchard, "The effects of hydraulic resistance on dam-break and other shallow inertial flows," J. Fluid Mech. **501**, 179 (2004).
[12] O. Pouliquen, "On the shape of granular fronts down rough inclined planes," Phys. Fluids **11**(7), 1956–1958 (1999).
[13] O. Pouliquen, "Scaling laws in granular flows down rough inclined planes," Phys. Fluids **11**(3), 542–548 (1999).
[14] O. Pouliquen and Y. Forterre, "Friction law for dense granular flows: Application to the motion of the motion of a mass down a rough inclined plane," J. Fluid Mech. **453**, 133–151 (2002).
[15] F. da Cruz, S. Emam, M. Prochnow, J.-N. Roux, and F. Chevoir, "Rheophysics of dense granular flows: Discrete simulation of plane shear flows," Phys. Rev. E **72**, 021309 (2005).
[16] P. Jop, Y. Forterre, and O. Pouliquen, "A constitutive relation for dense granular flows," Nature **44**, 727–730 (2006).
[17] T. Hatano, "Power-law friction in closely packed granular materials," Phys. Rev. E **75**, 060301(R) (2007).
[18] A. Fall, G. Ovarlez, D. Hautemayou, C. Mézière, J.-N. Roux, and F. Chevoir, "Dry granular flows: Rheological measurements of the $\mu(i)$-rheology," J. Rheol. **59**, 1065–1080 (2015).
[19] P. Jop, Y. Forterre, and O. Pouliquen, "Crucial role of sidewalls in granular surface flows: Consequences for the rheology," J. Fluid Mech. **541**, 167–192 (2005).
[20] P.-Y. Lagrée, L. Staron, and S. Popinet, "The granular collapse as a continuum: Validity of a navier-stokes model with a $\mu(i)$-rheology," J. Fluid Mech. **686**, 378–408 (2011).
[21] L. Staron, P.-Y. Lagrée, and S. Popinet, "Continuum simulation of the discharge of the granular silo," Eur. Phys. J. E **37**, 5 (2014).
[22] J. M. N. T. Gray and C. Ancey, "Segregation, recirculation and deposition of coarse particles near two-dimensional avalanche fronts," J. Fluid Mech. **629**, 387–423 (2009).
[23] K. Wieghardt, "Experiments in granular flow," Annu. Rev. Fluid Mech. **7**(1), 89–114 (1975).
[24] R. M. Iverson, "The physics of debris flows," Rev. Geophys. **35**(3), 245–296, doi:10.1029/97RG00426 (1997).
[25] A. Mangeney-Castelnau, J.-P. Vilotte, M.-O. Bristeau, B. Perthame, F. Bouchut, C. Simeoni, and S. Yerneni, "Numerical modeling of avalanches based on saint venant equations using a kinetic scheme," J. Geophys. Res. **108**(B11), 2527, doi:10.1029/2002JB002024 (2003).
[26] J. M. N. T. Gray and A. N. Edwards, "A depth-average μ(i)-rheology for shallow granular free-surface flows," J. Fluid Mech. **755**, 503–734 (2014).
[27] Here, the Froude number is arbitrarily defined as the velocity of the front non-dimensionalized by the characteristic velocity $\sqrt{g\,h\cos\theta}$, which is not equal to the wave speed in the framework of the propagating front.
[28] S. P. Pudasaini, "Some exact solutions for debris and avalanche flows," Phys. Fluids **23**, 043301 (2011).
[29] C. S. Campbell, "Rapid granular flows," Annu. Rev. Fluid Mech. **22**, 57 (1990).
[30] An asymptotic expansion of Eq. (17) for small values of H at the leading order of H leads to an exponential solution, as done in Ref. 26.
[31] Y. Forterre, "Kapiza waves as a test for three-dimensional granular flow rheology," J. Fluid Mech. **563**, 123–132 (2006).
[32] S. Deboeuf, E. Lajeunesse, O. Dauchot, and B. Andreotti, "Flow rule, self-channelization, and levees in unconfined granular flows," Phys. Rev. Lett. **97**, 158303 (2006).
[33] R. R. Kerswell, "Dam break with coulomb friction: A model for granular slumping," Phys. Fluids **17**, 057101 (2005).
[34] J. M. N. Gray, Y. C. T. Tai, and S. Noelle, "Shock waves, dead-zones and particle-free regions in rapid granular free-surface flows," J. Fluid Mech. **491**, 161–181 (2003).
[35] K. M. Hákonardóttir and A. J. Hogg, "Oblique shocks in rapid granular flows," Phys. Fluids **17**(7), 077101 (2005).
[36] A. Deboeuf, G. Gauthier, J. Martin, Y. Yurkovetsky, and J. F. Morris, "Particle pressure in a sheared suspension: A bridge from osmosis to granular dilatancy," Phys. Rev. Lett. **102**(10), 108301 (2009).
[37] F. Boyer, O. Pouliquen, and É. Guazzelli, "Dense suspensions in rotating-rod flows: Normal stresses and particle migration," J. Fluid Mech. **686**, 5–25 (2011).
[38] T. Dbouk, L. Lobry, and E. Lemaire, "Normal stresses in concentrated non-brownian suspensions," J. Fluid Mech. **715**, 239–272 (2013).
[39] T. Weinhart, A. R. Thornton, S. Luding, and O. Bokhove, "Closure relations for shallow granular flows from particle simulations," Granular Matter **14**(4), 531–552 (2012).
[40] A. Thornton, T. Weinhart, V. Ogarko, and S. Luding, "Multi-scale modeling of multi-component granular materials," J. Comput. Methods Mater. Sci. **13**(2), 1–16 (2013).
[41] L. E. Silbert, D. Ertaş, G. S. Grest, T. C. Halsey, D. Levine, and S. J. Plimpton, "Granular flow down an inclined plane: Bagnold scaling and rheology," Phys. Rev. E **64**(5), 051302 (2001).
[42] L. E. Silbert, J. W. Landry, and G. S. Grest, "Granular flow down a rough inclined plane: Transition between thin and thick piles," Phys. Fluids **15**(1), 1 (2003).
[43] H. Schlichting, *Boundary-Layer Theory*, 7th ed. McGraw-Hill Series in Mechanical Engineering (McGraw-Hill, New York, 1979).
[44] S. A. K. Mahady and L. Kondic, "A volume of fluid method for simulating fluid/fluid interfaces in contact with solid boundaries," J. Comput. Phys. **294**, 243–257 (2015).

Reuse of AIP Publishing content is subject to the terms at: https://publishing.aip.org/authors/rights-and-permissions. Downloaded to IP: 93.28.90.210 On: Tue, 17 May 2016 06:16:51

[45] E. Lerner, G. Düring, and M. Wyart, "A unified framework for non-Brownian suspension flows and soft amorphous solids," Proc. Natl. Acad. Sci. U.S.A. **109**(13), 4798–4803 (2012).
[46] E. Lajeunesse, A. Mangeney-Castelnau, and J. Vilotte, "Spreading of a granular mass on a horizontal plane," Phys. Fluids **16**(7), 2371–2381 (2004).
[47] D. Jessop, K. Kelfoun, P. Labazuy, A. Mangeney, O. Roche, J.-L. Tillier, M. Trouillet, and G. Thibault, "Lidar derived morphology of the 1993 lascar pyroclastic flow deposits, and implication for flow dynamics and rheology," J. Volcanol. Geotherm. Res. **245**, 81–97 (2012).
[48] L. Staron, P.-Y. Lagrée, C. Josserand, and D. Lhuillier, "Flow and jamming of a two-dimensional granular bed: Toward a nonlocal rheology?," Phys. Fluids **22**(11), 113303 (2010).
[49] S. Popinet, "Gerris: A tree-based adaptive solver for the incompressible euler equations in complex geometries," J. Comput. Phys. **190**(2), 572–600 (2003).

Reuse of AIP Publishing content is subject to the terms at: https://publishing.aip.org/authors/rights-and-permissions. Downloaded to IP: 93.28.90.210 On: Tue, 17 May 2016 06:16:51